



## AN EXPLORATION OF PARAMETRIC EARTHQUAKE RISK TRANSFER SOLUTIONS THAT DYNAMICALLY ADAPT TO SEISMICITY CHANGES

G. Franco<sup>(1)</sup>, R. Guidotti<sup>(2)</sup>, E. H. Field<sup>(3)</sup>, K. R. Milner<sup>(4)</sup>, Y. J. Lee<sup>(5)</sup>, and R. S. Stein<sup>(6)</sup>

<sup>(1)</sup> *Managing Director, Guy Carpenter, Guillermo.E.Franco@guycarp.com*

<sup>(2)</sup> *Cat Risk Research Analyst, Guy Carpenter, Roberto.Guidotti@guycarp.com*

<sup>(3)</sup> *Research Geophysicist, U.S. Geological Survey, Field@usgs.gov*

<sup>(4)</sup> *Computer Scientist, Southern California Earthquake Center, University of Southern California, kmilner@usc.edu*

<sup>(5)</sup> *Director, ImageCat Inc., yjl@imagecatinc.com*

<sup>(6)</sup> *CEO & Cofounder, Temblor, Ross@temblor.net*

### **Abstract**

(Re)insurance companies rely on earthquake risk models to estimate the frequency and severity of their potential financial losses. To protect themselves, they sometimes use parametric risk transfer solutions, which are derivative-form agreements that provide compensation as a function of routine measurable earthquake characteristics. These mechanisms typically remain in force for one to three years and assume seismic conditions—and our estimates of them—remain unchanged during this period. However, seismic risk estimates evolve continuously due to changes in nearby seismicity, sudden ruptures, slower redistributions of stress, or improvements in our own understanding of these phenomena. As a consequence, the likelihood of some loss-causing events might decrease and make the protection superfluous (wasted money), or, more problematically, it might increase and render the protection insufficient (increased risk).

This paper explores the construction of parametric earthquake risk transfer mechanisms that adapt efficiently (i.e., near real-time) to changes in seismicity throughout the lifetime of the transaction. The mechanism proposes the periodic adjustment of the payment conditions of the parametric agreement in harmony with the evolving probabilities of event occurrence. This, we hypothesize, may result in a more efficient allocation of premiums that reflects the changing nature of seismic risk.

To build the proposed dynamic risk transfer mechanism, we first employ one of the earthquake models commonly used in the (re)insurance industry to assess the risk of a portfolio of assets. The modeling exercise yields the expected frequency distribution of loss, which a standard (re)insurance transaction would typically consider constant for the entire coverage period. Here, we use these results simply as a baseline for the initial time step of reference. Next, we construct a retrospective update loop, which consists of two parts: (1) we obtain the earthquake occurrence rate conditions at a previous time step taking into account the changes in seismicity observed in the interim period; and (2) we use the modeled losses and adjusted frequencies at the new time step to build a parametric risk transfer solution. This parametric solution remains in force until it is updated at the next iteration. We also track the effects on the efficiency of the risk transfer solution and its premium if these continuous updates were not implemented.

We apply the proposed mechanism to California and find that changes in seismicity can cause swings in the frequency of parametric payments (which is related to the premium paid for the cover) in average of 16% and up to 36% in any three-year period from 1986 to 2020. We also find that avoiding an update of the parametric solution on a yearly basis to match the new risk profile can decrease the efficiency of the cover (measured as the relative contribution to the average annual loss of the events covered) in the same time period by 13% on average and up to 35%.

*Keywords: insurance; parametric; earthquake; dynamic; risk transfer*



## 1. Introduction

The (re)insurance industry is a sophisticated user of catastrophe risk models, which are numerical simulation platforms that estimate expected damages and losses derived from low probability events. As the historical record of such rare events is insufficient for any kind of actuarial approach, catastrophe risk models appeared in the 1980s as helpful tools to assist in the risk management and pricing operations of catastrophe insurance carriers [1, 2, 3]. The development and maintenance of these tools are costly and the investment decision as to whether to update a model hinges on market demand. Therefore, their evolution is rarely on par with the evolution of the risk they aim to depict, or the science they represent. In the absence of real-time models and often under the assumption that the modeled risks are tractable under a long-term lens, this divergence is to a large extent unavoidable. However, certain conditions exacerbate the discrepancy between the assumptions represented in the model and reality, which may lead to adverse consequences.

In this introduction, we point out the sources of misalignment between model and reality. We also summarize the main characteristics of parametric solutions and the mechanism chosen for this analysis. Section 2 describes the process proposed to create parametric earthquake solutions that adapt to seismicity changes. We present an application case study for California in section 3 and the conclusions of our work in section 4.

### 1.1 Sources of misalignment between model and reality

Catastrophe risk models consist of four fundamental components: hazard, vulnerability, exposure, and financial modeling. Those areas most directly affected by anthropogenic forces are the ones that are most likely to render a model outdated. For instance, changes to the building code might have the effect of rendering the damage functions of a model invalid for all exposures built after the enactment of such a code. The hazard component of a flood model may be highly dependent on whether levees are erected or removed. Risk models would be expected to accommodate such knowable changes to the built environment.

In this paper, we concern ourselves with one particular, perhaps trickier, aspect that may render an earthquake model an inaccurate representation of actual conditions: changes to the expected annual rate of events. In earthquake risk assessment, we are conscious that hazard conditions can change dramatically following a large event, but model developers may take some time to go through an update cycle. In the interim, users of such models are forced to continue using outdated or long-term hazard conditions, which they know no longer represent their risk profile. This was the case after the 2011 M9.0 Tohoku earthquake in Japan and the 2016 M7.8 Kaikoura earthquake in New Zealand, both of which altered risk conditions in Tokyo and Wellington, respectively. The Tohoku earthquake altered seismicity rates by factors of up to 100 at distances of up to 400 km from the M9.0 epicenter. The seismicity rate beneath Tokyo, for example, jumped by a factor of 10 at the time of the earthquake (Fig. 1). Almost a decade later, the seismicity rate beneath greater Tokyo is still higher than it was before 2011.

A faithful representation of reality would require a real-time assessment of hazard, vulnerability, and exposure conditions. This is what one could refer to as a “real-time” or “near-real-time” model. As those are not available yet, the analyses presented in this paper are limited to the effect of the annual event rates and their evolution through time, using mechanisms that do exist to estimate current event rates on a yearly basis. Other circumstances in which a misalignment might take place are induced not by the absence of an updated model but by the static nature of contractual agreements. In most traditional (re)insurance operations, agreements for coverage are renewed on a yearly basis. However, some instruments such as cat bonds or multi-year reinsurance agreements may remain in force for a duration of several years without alteration of the underlying assumptions employed at the onset of the contract. If in the interim span considerable changes in hazards occurred, the alignment of the coverage with the actual risk might suffer. In this work, we set out to obtain an approximate measure and correct for this misalignment in typical 1-5 year intervals.

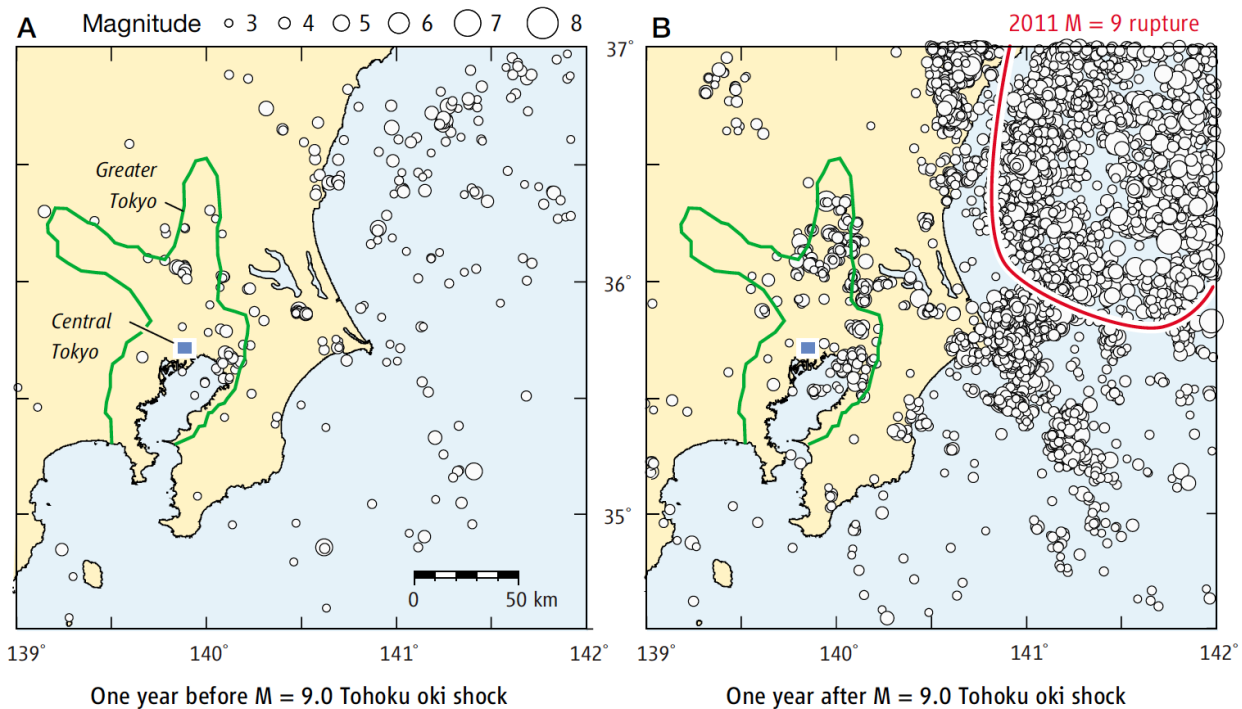


Fig. 1 – Seismicity shows about a 10-fold increase in annual quakes beneath greater Tokyo for the year after the M9.0 Tohoku earthquake (B) compared to the year beforehand (A), even though Tokyo lies well outside the rupture zone and traditional aftershock zone (delimited in red) of the main shock [4, 5].

## 1.2 Cat-on-a-grid parametric solutions

Most insurance transactions are executed on the basis of indemnity: the insurer is responsible to restore to the insured the value of the assets lost up to a pre-agreed limit and after subtraction of the agreed deductible (which has the purpose of reducing moral hazard and making the policy more affordable), all under a set of contractual policy obligations, conditions, and terms, and for a set of well-specified covered events. A claim made under an indemnity insurance policy requires that an assessment of the value lost be made by an expert. In the case of damages to a building experienced as a result of an earthquake, a contractor, engineer, or claims specialist carries out this assessment. This may take some time in a process that is often opaque to the insured and sometimes perceived as being fraught with difficulty and frustration.

Parametric solutions, first employed for earthquake risk covers in Japan in the 1990s and popularized later as a form of alternative earthquake insurance mechanism [6], aim to simplify this process by tying recoveries to the measurement of pre-agreed parameters such as a level of ground shaking intensity registered at a particular location or a level of moment magnitude of an earthquake occurring in a specified zone. A lot of creativity has been employed over the years in the (re)insurance industry to construct these types of solutions for earthquake risk transfer. This effort has given rise to payment trigger mechanisms such as ‘cat-in-a-box’ solutions, ground motion indices, and modeled loss triggers among others [7, 8], and some comparison exercises have been attempted to evaluate the performance of these solutions [9, 10, 11].

We have chosen to focus on one particular parametric insurance solution, often referred to as ‘cat-in-a-grid’ or ‘enhanced cat-in-a-box’ solution. This type of mechanism consists of defining a set of zones or ‘boxes’ arranged across a grid, where each grid cell has an associated magnitude threshold. If an earthquake occurred with its epicenter within a cell and its magnitude were equal to or higher than the cell’s threshold, a pre-agreed payment to the insured would take place. If depth is considered, the boxes become ‘cuboids’ and the focal depth becomes a relevant parameter in the transaction. These solutions evolved from considering a few zones like in the pioneering CAT-Mex transaction of 2006 [12] to hundreds or thousands like in the Acorn Re Ltd. 2015 cat bond [13] or in the Pacific Alliance transaction [14]. The evolution occurred thanks to a more intense computational effort devoted to solving this problem as well as to a greater tolerance in the financial markets



for adding some complexity in parametric transactions that helped increase their accuracy and reduce their basis risk (the difference between parametric payments and actual damages) [15, 16]. This simple typology of parametric transaction is easy to handle and to analyze and, for this reason, we chose it to illustrate a process of quantifying its performance and cost under time-dependent hazard conditions.

## 2. Methodology

The process followed in this paper consists of a retrospective loop represented in the flowchart of Fig. 2. We start from a baseline solution calculated with a commercially available earthquake risk model, as is routine in actual (re)insurance transactions. We then adjust the annual event rates in this model to reflect hazard conditions at different points in time retrospectively. This allows us to simply track the performance of the baseline solution, assuming it remains constant through time or change the solution to fit the risk profile at each time step. We describe in this section the steps required to perform these tasks.

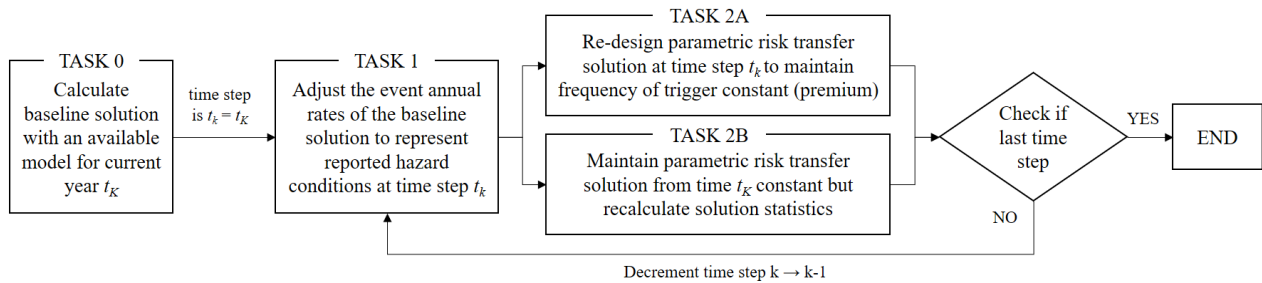


Fig. 2 – Iterative retrospective process.

### 2.1 Calculation of the baseline solution (TASK 0)

We consider a portfolio of assets subjected to seismic hazard, which we assume needs to be (re)insured via a parametric risk transfer solution. We assume that the year of interest is 2020, which we denote as our reference year  $t_k$ . To build this parametric solution, we employ a model that we assume to reflect hazard conditions at the reference year or the long-term average or ‘background’ state. We denote this initial parametric mechanism as the baseline solution. This first step requires the existence of a model that provides a stochastic set of earthquake events specifying their magnitude, the location of their focus, the expected loss  $L_i$  they produce, and their annual rate of occurrence, which we denote as  $r_i$ , for all simulated earthquakes  $i=1, 2, \dots, N$ .

To construct the cat-on-a-grid earthquake risk transfer solutions, we follow the approach presented in past illustrative applications for California [17] and Greece [18], which is based on maximizing the amount of risk transferred while ensuring that the annual trigger rate  $R$  (which determined the premium) remains under a specified value. This design philosophy aims to maximize recoveries for those types of earthquakes that are expected to pose a risk for the insured, either because they can cause a rare but large loss or because they cause moderate but frequent losses. However, the trigger frequency needs to be limited by the  $R$  constraint. Otherwise, the premium charged by the insurer, being a function of the trigger frequency, could be unaffordable. Stated as such, the combinatorial optimization takes the form of the classical knapsack problem formulation, which can be solved to find the best tradeoffs between coverage and cost. The problem can be expressed as:

$$\text{Maximize } \sum_{i=1}^N r_i L_i H(m_i - M_i) \text{ such that } \sum_{i=1}^N r_i H(m_i - M_i) \leq R \quad (1)$$

where  $H$  is the right-continuous (with  $H(0)=1$ ) Heaviside function, which takes a value of 1 for all events that have a magnitude  $m_i$  larger than or equal to their associated threshold magnitude  $M_i$  and therefore trigger the transaction. This optimization process results in a collection of magnitude thresholds  $M_i$  for each earthquake (or volume if depth is also a parameter) considered in the transaction.



## 2.2 Adjustment of the annual event rates (TASK 1)

We then consider hazard variations retrospectively. In particular, we assume that annual rates of occurrence of all earthquakes of interest can be assessed for all time steps  $t_k = t_0, t_1, \dots, t_K$ . Substituting the original annual rates at time step  $t_k$  for the corresponding annual rates at previous points in time, we can track two metrics retrospectively: 1) the efficiency of the trigger (i.e., the utility of the trigger to transfer loss in every one year) and 2) the frequency of payment of the trigger, which in turn is related to its technical premium (i.e., the cost of the policy or contract). We extend the nomenclature to express the annual event rates as  $r_{i,k}$ , where  $i$  denotes the event in the model and  $k$  the time step.

To simplify this exposition, we will assume henceforth that these annual rates of occurrence are obtained in their original form as  $r_{i,k}$ . This, however, is not exactly so in practice. Typically, the time-dependent annual rates will be obtained from a reporting source different than the one that produced the model, which means that the annual rates of events might not be exactly the same even for the same time step of reference  $t_k$ . This inconvenience is addressed by calculating the relative variation from the reporting source in each time step and applying this variation to the annual rates of the original model. We denote the annual event rates from the reporting source by  $r'_{i,k}$  and we can represent the changes in hazard from time step  $k$  to  $k-1$  by calculating the scalar factor  $a'_{i,k-1} = (r'_{i,k-1} - r'_{i,k}) / r'_{i,k}$ , which we use to approximate the annual event rates from the reference model  $r_{i,k-1}$  as the product  $a'_{i,k-1} r_{i,k}$ . Some numerical hindrances appear if the model or the reporting source have incomplete datasets with some rates equal to zero. For instance, if the annual rate in the model of reference is equal to zero, its value cannot be adjusted at all, as the product of the adjustment factor times the original rate is always zero. In our experiments, we found the numerical impact of those hindrances to be small as they affected only a few rare instances.

## 2.3 Parametric solution update (TASK 2A) and performance assessment (TASK 2B)

With the underlying event annual rates adjusted to represent hazard conditions at time step  $t_k$ , we have two choices with regard to the baseline parametric solution. We can either redesign this solution (TASK 2A) to maintain the original frequency of trigger constant and assess the fluctuation of its utility over time, or we can choose to maintain the baseline solution from time step  $t_k$  unaltered and simply track how utility and cost fluctuate over time (TASK 2B).

TASK 2B represents the status quo in the industry. When a parametric solution is computed in order to transfer the risk of a particular portfolio, this solution is maintained for the risk period considered, typically three years for most catastrophe bonds. So, in a “good” scenario, the maximum divergence between the hazard considered in the transaction and the actual hazard at any of the years during which the transaction is in force is limited to this interval. However, this situation is exacerbated if the model used does not represent actual conditions. For example, if a 2010 model is used to represent risk in 2020 to the risk period of 3 years, the 10-year age of the model would result in a total interval of 13 years.

We use two fundamental metrics to depict the performance of the parametric solution for each time step: (1) efficiency ( $E_k$ ) and (2) return period ( $T_k$ ), defined as:

$$E_k = \sum_{i=1}^N r_{i,k} L_i H(m_i - M_{i,k}) / \sum_{i=1}^N r_{i,k} L_i ; T_k = \left( \sum_{i=1}^N r_{i,k} H(m_i - M_{i,k}) \right)^{-1} \quad (2)$$

The numerator of the efficiency quotient is the average annual loss (AAL) of all events covered by the transaction while the denominator represents the AAL of all loss causing events, whether covered or not. A higher value of efficiency indicates that the parametric mechanism captures a high proportion of events contributing to the portfolio’s AALs, which is desirable. The return period is defined as the inverse of the annual trigger frequency, which should be close to  $R$  at the time of the design as this was a constraint imposed in the construction of the parametric trigger.

Adopting task 2A, i.e., redesigning the parametric transaction, involves solving the optimization problem again for the new annual occurrence rates but maintaining the original constraint on the total rates.



This will result in a set of magnitude thresholds  $M_{i,k}$  that change at every time step. The optimization aims to transfer as much risk as possible while maintaining the total trigger rate constant, which means the return period  $T_k$  will also be constant for all time steps, while the efficiency  $E_k$  will approach a maximum value at any time step  $k$ .

In contrast, adopting course of action 2B means we simply observe the evolution of the two metrics in time. As events will evolve differently in terms of their annual occurrence rates, it is *a priori* impossible to predict what impact this may have on trigger frequency and risk transfer. These metrics depend on the expected event losses and on the magnitude thresholds of the solution. Therefore, depending on the interplay of these parameters, efficiency and return period might increase or decrease. Precisely these variations illustrate the variation in performance we should expect to sustain if the annual occurrence rates are not a true depiction of actual conditions at every time step.

### 3. California Case Study

California is an area of interest for the (re)insurance community and for society at large. With a GDP of \$3 trillion, a population of 40 million people, and its high rate of seismicity, exposure to disruption from earthquakes is a great concern. Greater yet if one considers that the current residential insurance penetration rate is on the order of 10-15%. The need for financial protection is evident. Parametric solutions have been hailed as a device that could ameliorate this situation. The hope is that these types of tools, with their quick payout mechanism, their transparency, and their simplicity might persuade people to increase their insurance coverage. This is largely still an aspirational goal.

In this section, we consider a large, distributed portfolio of exposures in California—specifically, an estimate of the actual total building stock across the state—to construct a statewide parametric cover. The exposures are modeled with SeismiCat, which is ImageCat’s earthquake risk model and is briefly described in section 3.1. We then follow task 0 from the process described above, in order to construct a first baseline parametric solution. The modeled events’ annual occurrence rates are then updated as in the loop from Fig. 1 using retrospective data from a reporting source [19, 20], which includes both elastic rebound and spatiotemporal clustering (aftershock) time dependencies. Once the event rates are adjusted, we both (1) analyze how these rate changes would alter the performance of the baseline solution were it to remain static throughout the time period considered and (2) recalculate the parametric solution at each time to monitor what advantages that operation would yield in terms of utility to protect the exposures in terms of cost.

#### 3.1 Calculation of the baseline solution (TASK 0)

The model used for this case study is ImageCat’s SeismiCat. This model is a full-fledged stochastic earthquake loss model for earthquake risks in the U.S. consisting of hazard, exposure, and vulnerability components. SeismiCat uses an earthquake event catalog based on the Third California Earthquake Rupture Forecast (UCERF3) Time Dependent (TD) model [21]; this model includes elastic-rebound time dependence, but not spatiotemporal clustering (aftershocks), making it a long-term, time-dependent forecast.

Ground shaking intensity is modeled using empirical ground motion models (GMMs) from the Next Generation Attenuation-West2 (NGA-West2) developed by the Pacific Earthquake Engineering Research Center [22], consistent with the U.S. Geological Survey 2014 National Seismic Hazard Model (NSHM) [23]. The SeismiCat model rigorously treats both the epistemic and aleatory uncertainty in hazard models through earthquake simulations using a technology called Robust Simulation [24, 25, 26], in which model coherency and integrity are preserved throughout the loss calculation and integration process. In addition, both the between-event and within-event uncertainty in empirical GMMs as well as the spatial correlation of ground motion intensity are represented in SeismiCat’s event footprints. For modeling the seismic risks in California, the statewide  $V_s30$  map from the California Geological Survey [27] is used in modeling local site conditions



throughout the state. The soil response models are taken directly from each NGA-West2 GMM to account for local site effects.

SeismiCat utilizes the Code-Oriented Damage Assessment (CODA) model [28] to depict building damage as a function of building design parameters including natural vibration period, design base shear, and ductility. Seismic demand is taken as the spectral acceleration at the fundamental period. The model takes into account the evolution of building codes in the U.S. since 1935 to more accurately characterize California vulnerability considering buildings' lateral force systems, materials, heights, age, and municipality. This approach provides a framework for generalizing the ATC-13 damage functions and findings from more recent earthquakes (e.g., Northridge) and expanding implementation to more recent building construction practices.

The California exposure is modeled based on ImageCat's Inhance ITV (Insurance to Value) product and an Earth observation-derived building exposure dataset [29]. In general, the building exposure databases used for loss estimation in California are not adequate for identifying where economic loss is most likely because estimated replacement cost, a key factor in estimating potential financial consequences, is usually derived from very simplistic assumptions. Instead, the exposure model derives a more accurate estimate of cost, type, and spatial distribution of buildings from satellite imagery.

Applying the parametric design procedures introduced in section 2.1, we obtain the thresholds  $M_{i,k}$  that define the parametric solutions. As we group earthquakes according to their foci locations in a grid arrangement, the threshold conditions can be plotted on a map as in Fig 3.

Note that the parametric thresholds indicate two areas of high risk, namely the metropolitan areas of San Francisco and Los Angeles, where most of the California exposure is concentrated. The thresholds obtained in San Francisco, Los Angeles, San Diego, and Reno are, respectively, M7.3, M6.8, M7.5, and M8.6. The thresholds obtained for these large metropolitan areas are commensurate with the likelihood of experiencing large losses in California. For earthquakes occurring farther from the main areas of exposure concentration in Los Angeles and San Francisco, payments are triggered only if the magnitude is increasingly larger, as one would expect. This distribution of magnitude thresholds is a natural result of the optimization process, which tries to capture maximum risk while constraining the trigger frequency (as in the formulation of Eq. 1). In this case, the baseline parametric solution is computed assuming an annual trigger frequency of 1.33% which corresponds to a return period  $T_{2020}=75$  years.

### 3.2 Adjustment of the annual event rates (TASK 1)

In order to adjust the annual event rates of the baseline solution we use UCERF3 as the reporting source, which is actually composed of three different hierarchical models: (1) UCERF3-TI [30], which gives the long term rate of ruptures throughout the region, including those involving multiple faults; (2) UCERF3-TD [21], which adds long-term, time-dependent probabilities based on Reid's elastic rebound (i.e., time since last event on each fault); and (3) UCERF3-ETAS [19, 20], which adds spatiotemporal clustering (aftershocks) based on the Epidemic Type Aftershock Sequence model [31], in which every earthquake has a 5% to 15% chance of triggering something even larger. UCERF3-ETAS, which is used in this study, produces stochastic event sets of  $M \geq 2.5$  earthquakes for a specified timespan, conditioned on all  $M \geq 2.5$  events that occurred previously. As such, this is the first model that is capable of forecasting both aftershocks and finite, multi-fault ruptures.

### 3.3 Parametric solution update (TASK 2A) and performance assessment (TASK 2B)

In this part of the exercise, we proceed with tasks 2A and 2B within the retrospective iteration represented in Fig. 2. Task 2A consists of maintaining the return period of the parametric solution (its annual trigger frequency) constant and designing an optimal solution at each time step from 2020 back to 1986 such that it manages to capture as big a portion of the portfolio's AAL as possible for every year's hazard conditions. Task 2B consists of maintaining the baseline solution at  $t_k=2020$  constant and tracking the evolution of its performance metrics as we progress backwards in time. Fig. 4 shows the evolution of the return period of the



solution, its efficiency (i.e., the portion of the AAL associated with the covered events), and the total AAL contributed by covered and non-covered events.

For discussion, we assume that the premium that the insured paid in 2020 is somewhat proportional to the frequency of trigger payments. The more often the trigger pays, the costlier the insurance policy (while this is in general true, in reality this is a nonlinear relationship that involves assessing the cost of capital under varying market conditions). Two scenarios are at opposing ends of a spectrum: (1) the insured will be in an undesirable position in years when the trigger return period increases (frequency decreases and they would be overpaying based on their 2020 premiums); and (2) the efficiency of the trigger to transfer loss decreases (they are getting less utility from the cover than they got in 2020). Conversely, the insured is in a beneficial position when the trigger return period decreases (frequency increases and they are underpaying based on their 2020 premiums) while the efficiency increases (they are getting more utility than expected).

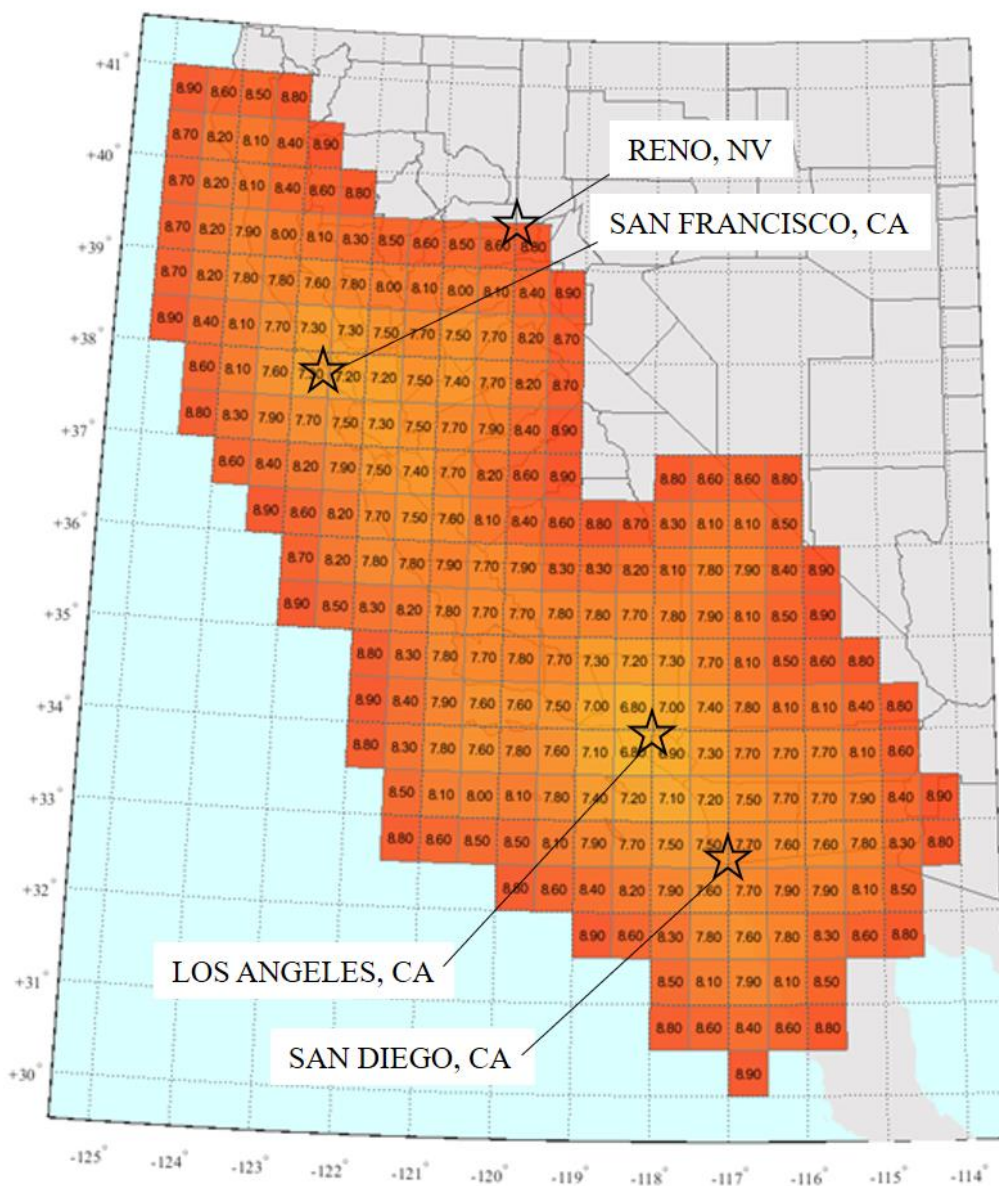


Fig. 3 – Baseline parametric solution for California based on the underlying SeismiCat model and optimized to provide maximum risk coverage at an estimated return period of 75 years.



Following task 2A, we observe that the return period (Fig. 4 upper left plot) remains constant. This is to be expected as the return period is the inverse of the total trigger rate, which is constrained to a fixed value  $R$  in the optimization process. As this optimization is carried out at each time step, the return period does not vary. The efficiency of the trigger (Fig 4. bottom left plot) varies, however, depending on the result of the optimization problem. Recall that the aim of the optimization at each time step is to set the magnitude thresholds in such a manner that the events that trigger the transaction are those responsible for the highest possible proportion of AAL without violating the total annual rate constraint. The variations up and down in efficiency are therefore due to the fact that overall changes in event rates might make it harder or easier at each time step to achieve this maximization objective.

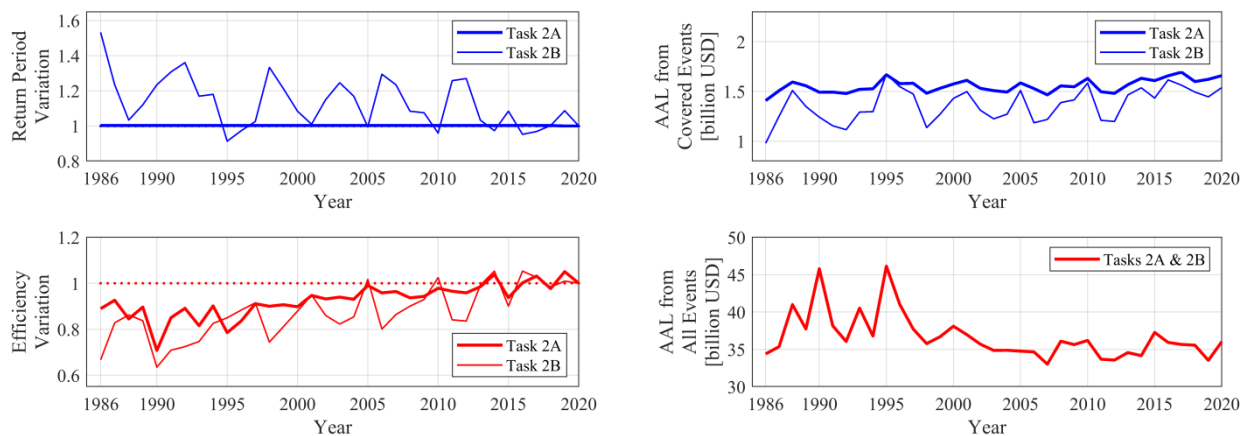


Fig. 4 – Retrospective performance evolution for task 2A (left) & 2B (right).

Following task 2B, we observe a decreasing trend in the return period going forward in time. This means the annual rate of trigger payments evolves from about 1-in-115-years back in 1986 (a factor of about 1.5 with respect to 2020) to 1-in-75-years in 2020. This suggests that there has been an increase in expected annual occurrence rates for those earthquakes covered by the baseline solution (which remains static in this exercise). During the same period, the efficiency of the trigger, its ability to transfer risk, grows from 1986 to its optimal design value in 2020. Efficiency and the AAL from covered events following task 2B are generally suboptimal with respect to task 2A. Observe how in the upper right plot of Fig. 4 the AAL from covered events for course of action 2A is always superior to that of course of action 2B. This, again, is natural, as task 2A maximizes this metric at every step, but with 2B we simply track the performance of a static solution that was optimized only once for the reference year 2020.

These general trends mask some particular instances that reveal the true impact of changing hazard conditions on a static parametric risk transfer solution. In particular, some years show a large increase in return period, which translates into a decrease in trigger frequency and therefore into a lower premium. Take for example, year 2012 in which the return period increased by 27% with respect to 2020 in the task 2B column of Table 1. That means that the premium paid in 2020 represented an estimated overpayment of 21% (from  $1 - 1.27^{-1}$ ) with respect to the actual premium that should have been paid in 2012. While this occurred, the efficiency of the parametric transaction in 2012 dropped by 16%. Therefore, if the same policy had been static over a period of 8 years (or the model had not been updated during that time), the insured would be subjected to a potential swing in premiums of 21% and a drop in utility of the cover of 16%. These are not small swings, but the period of time is considerable. If we had instead reoptimized for the actual annual event rates, as per task 2A, the frequency of trigger (and therefore premium) would have remained the same and efficiency would have dropped only by a small percentage of 4%.

The year-to-year differentials can be dramatic in some years of increased seismic activity. Note the change in return periods in task 2B between 1994 (Northridge) and 1995, which translates into a trigger frequency (premium) delta of 25% while the relative efficiency change is limited to 2%. In other words, this



reflects a situation in which the cover's utility for a two-year period is nearly constant but whose price changes by 25% depending on the year in which it is issued. Considering all three-year periods (the typical risk period of a cat bond transaction) from 1986 to 2020, we find that changes in seismicity cause, on average, swings in the frequency of parametric payments of 16% and up to 36% if the parametric solution is not updated yearly. This can also decrease the efficiency of the cover in the same time period by 13% on average and up to 35%.

Table 1 – Return period and efficiency variation as well as average annual loss (AAL) from covered events and from all the events for selected years in the sample according to the two tasks considered.

Year	Task 2A			Task 2B			AAL from all Events [Billion USD]
	Return Period Variation	Efficiency Variation	AAL from Covered Events [Billion USD]	Return Period Variation	Efficiency Variation	AAL from Covered Events [Billion USD]	
2020	1.00	1.00	1.66	1.00	1.00	1.54	36.02
2012	1.00	0.96	1.48	1.27	0.84	1.20	33.57
1995	1.00	0.79	1.67	0.91	0.85	1.67	46.13
1994	1.00	0.90	1.53	1.18	0.83	1.30	36.78
1993	1.00	0.82	1.52	1.17	0.75	1.29	40.52

#### 4. Conclusions

Near-real-time risk models are progressively becoming available in government and commercial means, which makes the construction of risk transfer tools reflective of current conditions at any given time an exciting prospect for the (re)insurance industry. Use of these models could make the market more responsive and liquid. Some new tools are appearing that target critical portions of cat risk models, the hazard, in particular. Realtime Risk, one of such tools developed by Temblor Inc. [[www.temblor.net](http://www.temblor.net)] captures these changes in seismicity based on Coulomb stress transfer theory. Similarly, efforts within the domain of Operational Earthquake Forecasting [32] can progressively inform the development of risk assessments closer to real-time, as exemplified in previously developed prototypes [33].

We have shown that taking such seismicity changes into account on a yearly basis and redesigning the risk cover to match the new risk profile leads to stable pricing conditions and optimal utility of the cover at any given time. The impacts of failing to consider the changes in seismicity in risk transfer transactions have been found to be significant for California, and almost certainly will be more so in Japan and Chile, where large earthquakes near population centers are more frequent. We expect that highly concentrated portfolios will be much more susceptible to the swings in performance we have shown for a widely distributed portfolio across California. And were we to focus on time periods around large shocks, we might see these effects emphasized once again.

In essence, a more complete and rigorous study of these effects might be useful to establish clear guidance as to what situations should be avoided before structuring large transactions lest the risk cover be subjected to large variations in its performance and ultimate value to the insured.

#### 5. Disclaimer

Any use of trade, firm, or product names is for descriptive purposes only and does not imply endorsement by the U.S. Government.



## 6. References

- [1] Grossi P, Kunreuther H (2005): Catastrophe modeling: A new approach to managing risk. Huebner international series on risk, insurance and economic security. Springer.
- [2] Mitchell-Wallace K, Jones M, Hillier J, Foote M (2017): Natural catastrophe risk management and modelling: A practitioner's Guide. John Wiley & Sons.
- [3] The Geneva Association (2018): Managing physical climate risk: Leveraging innovations in catastrophe risk modelling. Published by The Geneva Association-International Association for the Study of Insurance Economics.
- [4] Toda S, Stein RS (2013): The 2011 M = 9.0 Tohoku oki earthquake more than doubled the probability of large shocks beneath Tokyo, *Geophys. Res. Letts.*, 40, doi:10.1002/grl.50524.
- [5] Stein RS, Toda S (2013): Megacity megaquakes—Two near misses, *Science*, 341, 10.1126/science.1238944
- [6] Franco G (2014): Earthquake mitigation strategies through insurance. In *Encyclopedia of Earthquake Engineering*, pp. 1-18. Springer Berlin Heidelberg.
- [7] Wald DJ, Franco G (2016): Money matters: Rapid post-earthquake financial decision-making. *Natural Hazards Observer*, 40 (7), 24-27.
- [8] Wald DJ, Franco G (2017): Financial decision-making based on near-real time earthquake information. In *Proceedings of the 16th World Conference on Earthquake Engineering*, Santiago.
- [9] Goda K (2013): Basis risk of earthquake catastrophe bond trigger using scenario-based versus station intensity-based approaches: A case study for southwestern British Columbia. *Earthquake Spectra*, 29(3):757–775.
- [10] Goda K, Franco G, Song J, Radu A (2019): Parametric catastrophe bonds for tsunamis: Cat-in-a-box trigger and intensity-based index trigger methods. *Earthquake Spectra*, 35(1):113–136.
- [11] Pucciano S, Franco G, Bazzurro P (2017): Loss predictive power of strong motion networks for usage in parametric risk transfer: Istanbul as a case study. *Earthquake Spectra*, 33(4):1513–1531.
- [12] Cardenas V, Hochrainer S, Mechler R, Pflug G, Linnerooth-Bayer J (2007): Sovereign financial disaster risk management: The case of Mexico. *Environ. Haz.*, 7:40–53.
- [13] Artemis (2015): Acorn Re Ltd. (Series 2015-1). <https://www.artemis.bm/deal-directory/acorn-re-ltd-series-2015-1/>, last accessed Feb 2020.
- [14] Artemis (2018): Pacific Alliance cat bond to settle at USD 1.36bn, priced below guidance. <http://www.artemis.bm/blog/2018/02/05/pacific-alliance-cat-bond-to-settle-at-1-36bn-priced-below-guidance/>, last accessed Feb 2020.
- [15] Franco G (2010): Minimization of trigger error in cat-in-a-box parametric earthquake catastrophe bonds with an application to Costa Rica. *Earthquake Spectra*, 26 (4), 983-998.
- [16] Franco G (2013): Construction of customized payment tables for cat-in-a-box earthquake triggers as a basis risk reduction device. In *Proc. of the International Conf. on Structural Safety and Reliability (ICOSSAR)*, 5455-62.
- [17] Franco G, Tirabassi G, Lopeman M, Wald DJ, Siembieda WJ (2018): Increasing earthquake insurance coverage in California via parametric hedges. In *11th US National Conference on Earthquake Engineering*, Los Angeles.
- [18] Franco G, Guidotti R, Bayliss C, Estrada-Moreno A, Juan AA, Pomonis A (2019): Earthquake financial protection for Greece: A parametric insurance cover prototype. In *Proceedings of the ICONHIC2019 2nd International Conference on Natural Hazards and Infrastructure*, pages 1–8, Chania, Greece.
- [19] Field EH, Milner KR, Hardebeck JL, Page MT, van der Elst N, Jordan TH, Michael AJ, Shaw BE, Werner MJ (2017): A spatiotemporal clustering model for the Third Uniform California Earthquake Rupture Forecast (UCERF3-ETAS): Toward an operational earthquake forecast, *Bull. Seism. Soc. Am.* 107, 1049–1081, doi: 10.1785/0120160173.
- [20] Field EH, Jordan TH, Page MT, Milner KR, Shaw BE, Dawson TE, Biasi GP, Parsons T, Hardebeck JL, Michael AJ, Weldon II RJ, Powers PM, Johnson KM, Zeng Y, Bird P, Felzer KR, van der Elst N, Madden C, Arrowsmith R, Werner MJ, Thatcher WR, Jackson DD (2017): A synoptic view of the Third Uniform California Earthquake Rupture Forecast (UCERF3), *Seismol. Res. Lett.*, 88, doi: 10.1785/0220170045.



- [21] Field EH, Biasi GP, Bird P, Dawson TE, Felzer KR, Jackson DD, Johnson KM, Jordan TH, Madden C, Michael AJ, Milner KR, Page MT, Parsons T, Powers PM, Shaw BE, Thatcher WR, Weldon II RJ, Zeng Y (2015): Long-term, time-dependent probabilities for the Third Uniform California Earthquake Rupture Forecast (UCERF3), *Bull. Seismol. Soc. Am.* 105, 511-543, doi: 10.1785/0120140093.
- [22] PEER (2013): <https://peer.berkeley.edu/research/nga-west-2/final-products>.
- [23] Petersen MD, Moschetti MP, Powers PM, Mueller CS, Haller KM, Frankel AD, Zeng Y, Rezaeian S, Harmsen SC, Boyd OS, Field EH, Chen R, Rukstales KS, Luco N, Wheeler RL, Williams RA, and Olsen A (2014): Documentation for the 2014 update of the United States national seismic hazard maps: U.S. Geological Survey Open-File Report 2014-1091, 243 p., <https://dx.doi.org/10.3133/ofr20141091>.
- [24] Taylor CE (2015): *Robust simulation for mega-risks - The path from single solutions to competitive, multi-solution methods for mega-risk management*, Springer International Publishing, ISBN 978-3-319-19413-4, October 2015.
- [25] Lee YJ, Graf W, Hu Z (2018): Characterizing the epistemic uncertainty in the USGS 2014 National Seismic Hazard Mapping Project (NSHMP). *Bull. Seismol. Soc. Am.*, Vol. 108, No. 3A, pp. 1465-1480
- [26] Lee YJ (2018): Catastrophe loss modeling through Robust Simulation, in proceedings, Eleventh U.S. National Conf. on Earthquake Engineering, Los Angeles, California, 25-29 June 2018.
- [27] Wills CJ, Gutierrez CI, Perez FG, and Branum DB (2015): A next-generation Vs30 map for California based on geology and topography. *Bull. Seismol. Soc. Am.*, 105 (6): 3083-3091.
- [28] Graf WP, Lee Y (2009): Code-Oriented Damage Assessment for buildings. *Earthquake Spectra* 25(1), pp. 17-37.
- [29] ImageCat, Inc. (2020). Inhance® ITV [database]. ImageCat, Inc., Long Beach, CA.
- [30] Field EH, Arrowsmith RJ, Biasi GP, Bird P, Dawson TE, Felzer KR, Jackson DD, Johnson KM, Jordan TH, Madden C, Michael AJ, Milner KR, Page MT, Parsons T, Powers PM, Shaw BE, Thatcher WR, Weldon RJ, Zeng Y (2014): Uniform California Earthquake Rupture Forecast, version 3 (UCERF3)—The time-independent model, *Bull. Seismol. Soc. Am.*, 104, 1122-1180, doi: 10.1785/0120130164.
- [31] Ogata Y (1988): Statistical models for earthquake occurrences and residual analysis for point processes. *J. Am. Stat. Assoc.* 83, 9-27.
- [32] Field EH, Jordan TH, Jones LM, Michael AJ, Blanpied ML, Other Workshop Participants (2016): The potential uses of Operational Earthquake Forecasting, *Seismol. Res. Lett.* 80, 1-10. doi: 10.1785/0220150174.
- [33] Field EH, Porter K, Milner K (2017): A prototype operational earthquake loss model for California based on UCERF3-ETAS – A first look at valuation, *Earthquake Spectra*, 33, 1-21, doi: 10.1193/011817EQS017M. IP-087973.